Electronic Supplementary Material (ESI) for Journal of Materials Chemistry A.

Supporting Information:

The Growth Mechanism of Lithium Dendrites and its Coupling to Mechanical Stress

Julian Becherer, Dominik Kramer*, and Reiner Mönig

Institute for Applied Materials, Karlsruhe Institute of Technology,
Hermann-von-Helmholtz-Platz 1, 76344 Eggenstein-Leopoldshafen, Germany
* Corresponding author: dominik.kramer@kit.edu

This Supporting Information contains four additional figures (S1-S4). In Section A1, EDX data with maps for oxygen and carbon is displayed (Figure S1). Results from the growth of needles and loops at a current density of −0.5 mA cm^{-2} are shown in Section A2 with the length vs. time development (Figure S2) and light microscopy images of a loop (Figure S3). The Section A3 is a more detailed discussion of the dependencies of length vs. time compared with the ionic depletion as described by calculated concentrations vs. time. In Section A4 a schematic of the atom insertion at the edge dislocation at an extra half-plane is shown (Figure S4).

Further Supporting Information is contained in four mp4 video files (SV1 to SV4):

- SV1 needle growth at −0.05 mA cm^{-2}
- SV2 loop growth at −0.05 mA cm^{-2}
- SV3 EBSD patterns for various measurement points on a kinked loop.
  See explanatory on the next page.
- SV4 loop growth at −0.5 mA cm^{-2}

Explanatory note

In video SV3, an SEM image of a loop is depicted together with the Kikuchi patterns recorded at different positions. The green square in the SEM image indicates the electron beam position of the corresponding Kikuchi pattern displayed on the right. Lithium has little interaction with electrons, and therefore, the backscattered intensity is very low and the diffraction patterns exhibit noise. Nevertheless, lines are discernable, which indicate crystallinity. The orientation of the lines correlates with the orientation of the reciprocal lattice and hence can be used to indicate the orientation of different regions of the loop. The fact that the diffraction patterns change before and after kinks show that the crystal orientations change, which clearly indicates that there must be grain boundaries between the diffraction spots. Points with the same lattice orientation are designated with the same letter (a, b, c, d).

A1. Chemical composition of the surface on lithium structures grown at −0.05 mA cm^{-2}

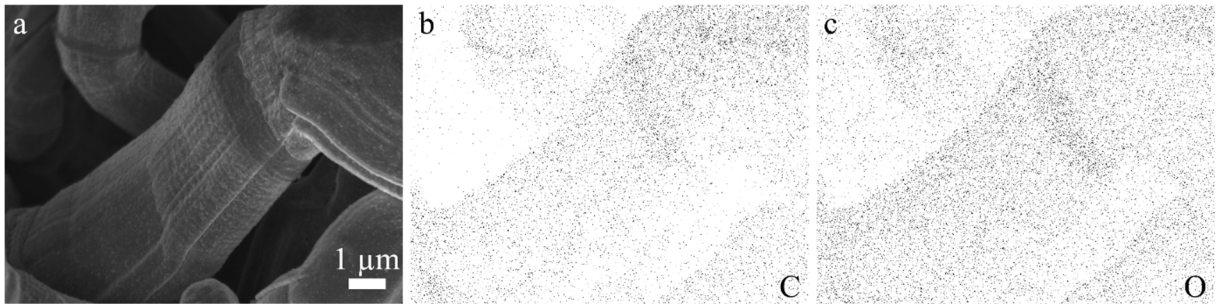

Figure S1. Investigation of the chemical composition by EDX. (a) SEM image, (b) map of the carbon distribution, and (c) map of the oxygen distribution**.**

A2. Growth at −0.5 mA cm^{-2}

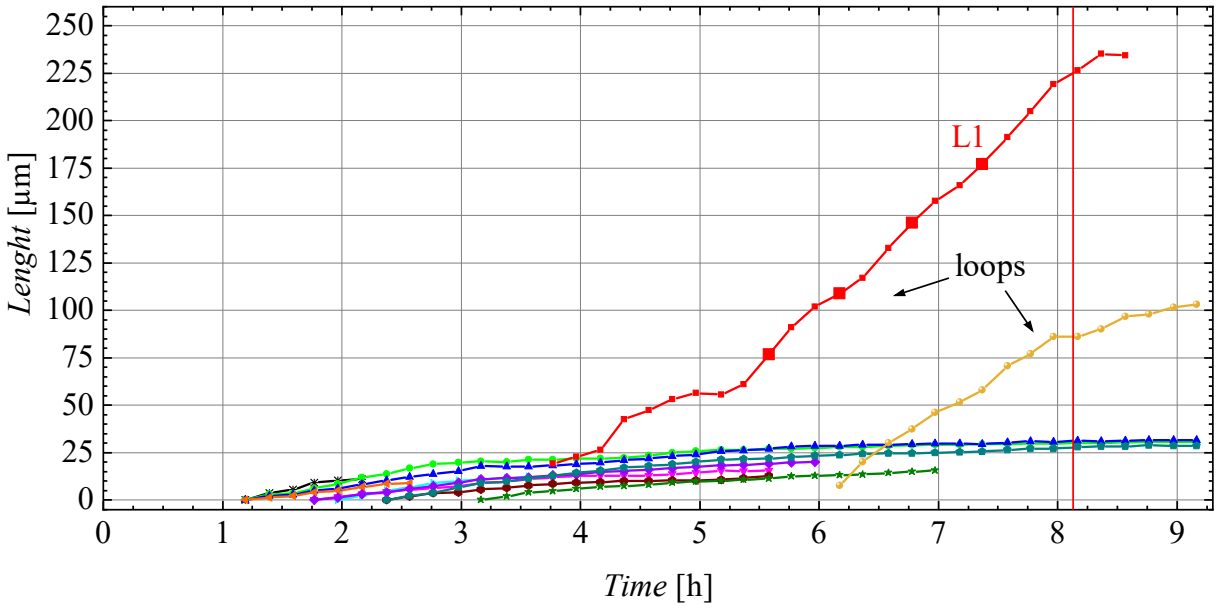

Figure S2. Length development of ten needles and two loops during the lithium electrodeposition at −0.5 mA cm^{-2}. Large symbols for the loop L1 indicate when the images in Figure S3 were taken. The red vertical line indicates the initiation of a fast growing bush dominating the deposition.

Figure S2 shows the development of the length of ten needles and two loops during the deposition at −0.5 mA cm^{-2}. The evaluated needles initiated between ~1 h and 10 min and ~3 h and 10 min

after the pretreatment was completed. They stopped to grow at total needle lengths varying between 9 µm and 32 µm, which is significantly shorter than the needles that grew at −0.05 mA cm^{-2}. The loops initiated later during the deposition, and they could be observed for shorter loop length than the loops grown at −0.05 mA cm^{-2} since the needles blocking the view were shorter. Both loops grow considerably faster than the needles. Both loops reduce the growth rate significantly after approximately 8 hours, which is in good agreement with the initiation of a fast growing bush that dominates the deposition (indicated by the red vertical line). The initiation of such fast growing bushes was investigated in more detail in our previous work.[1] Figure S3 shows four images

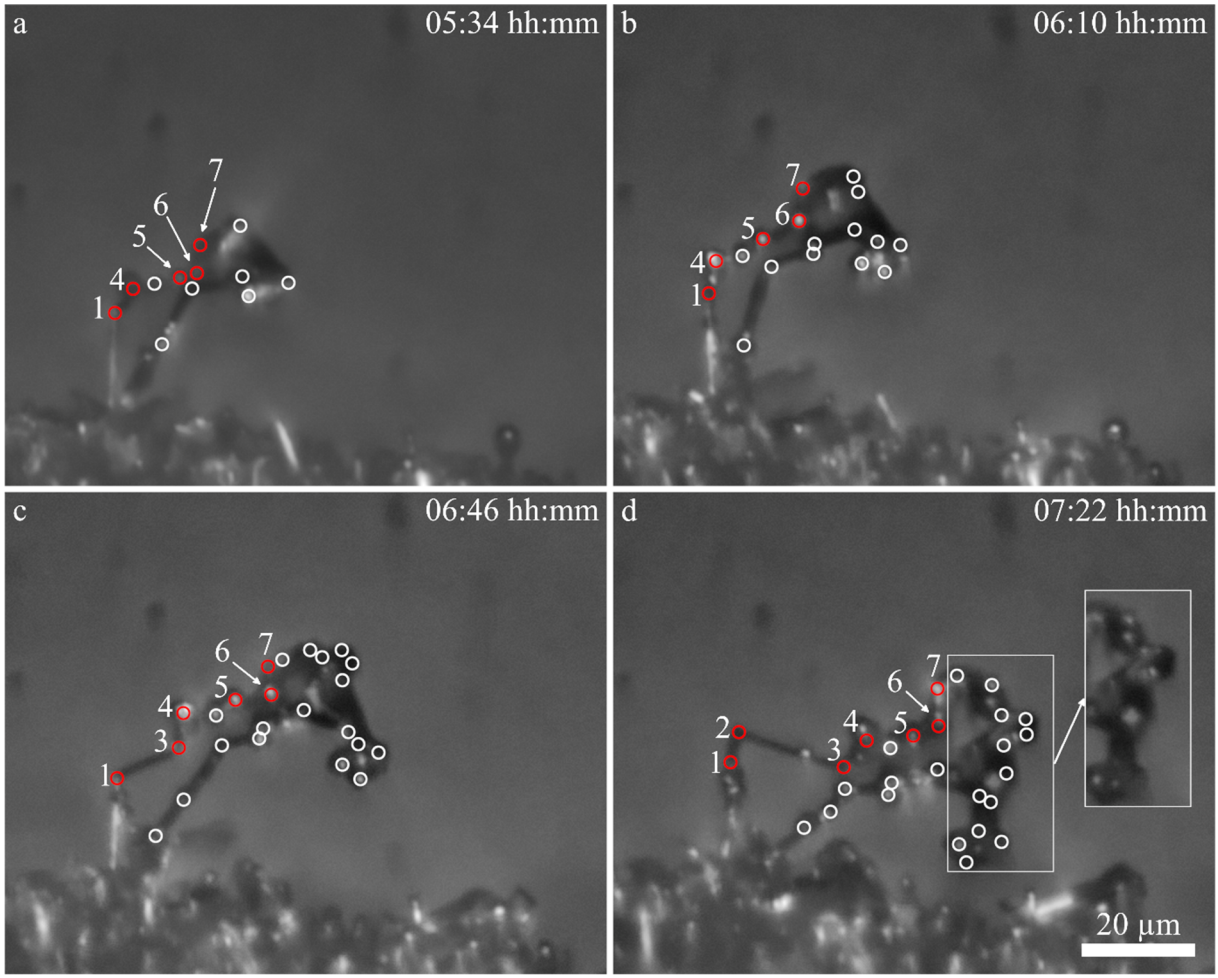

Figure S3. (a-d) Growth of the lithium loop L1 at −0.5 mA cm^{-2} with 36 min of deposition between the images. White circles indicate kinks of the loop; red circles indicate the numbered kinks that are referred to in the text. The number of kinks increases over time. The inset in (d) shows a part of the loop with no marks for a better visibility of the bulges. The larger symbols in the L1-plot of Figure S2 indicate when the images (a-d) where taken.

of the loop L1. The large symbols of the L1-plot in Figure S2 indicate when the images in Figure S3 were taken. Both ends of the loop are attached to the substrate in locations very close to each other. The right segment leading to the substrate rotates clockwise between Figure S3c and d, but the end of this segment seems still to end at its initial position (view on the ends is blocked by surrounding needles). This indicates that the connection the substrate was stable throughout the observed loop growth. The segments between the numbered kinks 5 to 7 hardly grow during the deposition. Between the first two images, the segment between kink 1 and 4 also hardly changes, but after the new kinks 3 and 2 are formed, significant growth occurs at these insertion sites. In the right part of the loop, a large number of new kinks continuously form but hardly any long segments grow. At most of these kinks, bulges occur. These bulges are better visible in the inset in Figure S3d with no markers.

A3. Discussion of length vs. time and concentration vs. time dependencies

It has been shown by Nishikawa et al.[2,3] that for lithium deposition in propylene carbonate electrolytes there is a linear dependence of the length l of bushes vs. the square root of time $\sqrt{t}$, at various current densities. Therefore, the length can be described as

$$l = b\sqrt{t} - l_0 \qquad (1)$$

This experimental result might be useful for a phenomenological description of bush growth. It is likely that physical effects cause the behavior observed. For example, the growing needles might kink from time to time in random directions. This might cause a growth where the tip moves in a similar way than a random walk. This would result in a mean travel distance of the needle tip, which is a function of $\sqrt{t - t_0}$, with the time t_0 for the initiation of the needle growth:

$$l = b\sqrt{t - t_0} \qquad (2)$$

This is an example of a $\sqrt{t}$ dependence that does not imply any relation to the diffusional transport in solution.

For a galvanostatic experiment with metal deposition on a flat electrode, the metal ion concentration at the surface c_S is given by.[2,3]

$$c_S = c_0 - \frac{2j(1-\tau)}{zF\sqrt{\pi D}}\sqrt{t} = c_0 - B\sqrt{t}, \qquad (3)$$

with the initial concentration c_0, the current density j, the transference number τ, Faraday's constant F, the charge of the ion z, and the diffusion parameter D. Similar to Equation (1), Equation (3) has a square-root dependence on the time, but with a negative sign. Equation (1) describes the length, Equation (3) the concentration. Length and concentration have no direct relation, but the length change $\frac{dl}{dt}$ is proportional to the local current density j, which depends on the local concentration of lithium ions. In the general case, j will be a function of the concentration c of the ions according to $j = F\,k\,c^{\alpha}$, with the transfer coefficient α.[4] Here, we consider two special cases, $\frac{dl}{dt} = k\,c_S$ and $\frac{dl}{dt} = k\sqrt{c_S}$, i.e. we assume that the relevant concentration in the solution close to the growing dendrite can be approximated by the concentration at a flat electrode as given by Equation (3). Since a galvanostatic deposition is considered, the exact potential is not constant, and any reduction of a local current, e.g. due to a decreasing concentration, must be balanced by a larger current elsewhere, e.g. by the nucleation of a new needle.

If we assume that the local growth rate would be proportional to the surface concentration $\frac{dl}{dt} = kc_S = k\left(c_0 - B\sqrt{t}\right)$, the length of the bush is obtained as

$$l = k\,c_0\,t - \frac{2}{3}k\,B\,t\sqrt{t} = k\,t\left(c_0 - \frac{2}{3}\,B\sqrt{t}\right) - l_0\,. \qquad (4)$$

If we consider a more realistic value of the symmetry factor α, α = 0.5, the lithium growth rate will depend on the root of the ionic concentration close to the surface,[5] and we obtain $\frac{dl}{dt} = k\sqrt{c_S} = k\sqrt{c_0 - B\sqrt{t}}\,.$

Integration results in

$$l = \frac{4\,k}{15\,B^2}\left\{2\,c_0^{\frac{5}{2}} - \left(c_0 - B\sqrt{t}\right)^{\frac{3}{2}}\left(3\,B\sqrt{t} + 2\,c_0\right)\right\} - l_0. \qquad (5)$$

The empirical Equation (1) for the length differs from the theoretical equations (4) and (5), in particular with respect to the behavior at $t = 0$ where Equation (1) implies an infinite slope whereas (4) and (5) suggest a finite one. However, due to the nucleation time, which is included indirectly in the equations by the l_0 terms, the behavior of the curve close to $t = 0$ is hidden. Due to the

variation that is present in the growth of lithium structures, including nucleation time and growth angle variations, length vs. time plots have an inherent considerable scatter. The "random walk of the dendrite tips" as described by Equation (2) and the "concentration determines growth rate" models as given by Equations (4) and (5) result in curves which can hardly be discriminated by the fit quality of corresponding length vs. time $l(t)$ curves on the experimental results.

As discussed above, it has been suggested that the needles decelerate due to the decreasing concentration of the solution.[2,3] To keep the galvanostatic current, more needles have to nucleate then. We suggest that the mechanism might be the other way around: The nucleation of new needles is progressive. Both the nucleation of more and more needles and bushes and the growing lithium surface area cause a decrease in the local current density of a given needle. Correspondingly, the growth at the individual sites slows down. This should be independent of ionic concentrations; we observe the deceleration of needles (Figure 1 and Figure S2) for small currents in a cell with convection where the ionic depletion effect is not pronounced. For a smaller local growth rate, the continuous dispersion of the SEI over the growing surface is less effective, the SEI can grow thicker at and close to the nucleation sites. This growing SEI might also contribute to the growth deceleration. If the SEI is thick enough to impede most of the growth locations, the transition of the growth to a fast-growing bush can occur suddenly, as described in our previous publication.

According to our observations, at least four growth regimes exist. They differ in morphology and growth rate. In the order of increasing growth rate these are needles, loops, bushes and fast growing bushes; this order is also the order in deposition time at which these structures occur. This sequence results in a complex dependence position of the outmost tip of the structure on the time.

A4. Insertion at an extra half-plane resulting in growth along the Burgers vector

The lower part of Figure S4 shows the insertion mechanism of atoms at the edge dislocation of an extra half-plane. This is a negative type of dislocation climb. Negative climb requires the diffusion of atoms to the dislocation line (vacancy diffusion away from the dislocation). Since vacancies diffuse from tensile regions to compressive regions, the dislocation line has to be more tensile than other region in the crystal for this diffusion to take place. From thin film growth, it is known that the diffusion of adatoms into GB generates extremely high compressive stresses[6,7] and hence it is likely that the vacancies in the lithium loops diffuse from dislocation lines to GBs.

This corresponds to the motion of atoms from the GB to the insertion site at the dislocation line. In Figure S4, the atoms at the lower edge of the plane are inserted subsequently. In the last illustration on the right, the plane reaches the surface of the crystal and hence the defect is healed and a full new plane has grown. This results in a growth of one lattice plane along the Burgers vector $\vec{b}$, which corresponds to a ⟨111⟩ direction in bcc crystals. Plasticity due to the growth stresses may continuously generate new defects of this type, facilitating the growth in this direction.

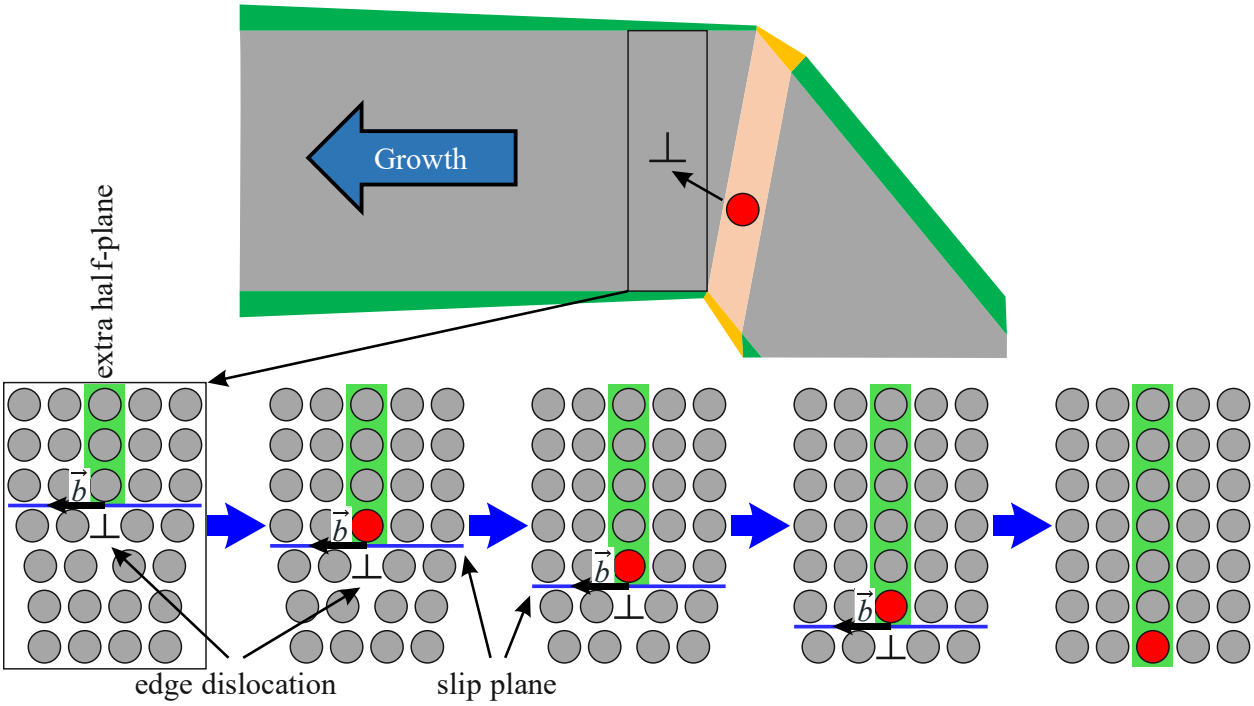

Figure S4. Schematic illustration of growth by a negative climb of edge dislocations. The inserted atoms at the edge dislocation are highlighted in red, the slip plane is indicated by a blue line, and the extra half-plane is highlighted in green.

References

[1] J. Becherer, D. Kramer, R. Mönig, *ChemElectroChem* **2021**, *8*, 3882–3893.

[2] K. Nishikawa, T. Mori, T. Nishida, Y. Fukunaka, M. Rosso, T. Homma, *J. Electrochem. Soc.* **2010**, *157*, A1212.

[3] K. Nishikawa, T. Mori, T. Nishida, Y. Fukunaka, M. Rosso, *J. Electroanal. Chem.* **2011**, *661*, 84–89.

[4] W. Schmickler, E. Santos, *Interfacial Electrochemistry*, Springer Berlin Heidelberg, Heidelberg, Germany, **2010**.

[5] L. Mishra, A. Subramaniam, T. Jang, K. Shah, M. Uppaluri, S. A. Roberts, V. R. Subramanian, *J. Electrochem. Soc.* **2021**, *168*, 092502.

[6] E. Chason, B. W. Sheldon, L. B. Freund, J. A. Floro, S. J. Hearne, *Phys. Rev. Lett.* **2002**, *88*, 156103.

[7] J. Leib, R. Mönig, C. V. Thompson, *Phys. Rev. Lett.* **2009**, *102*, 256101.